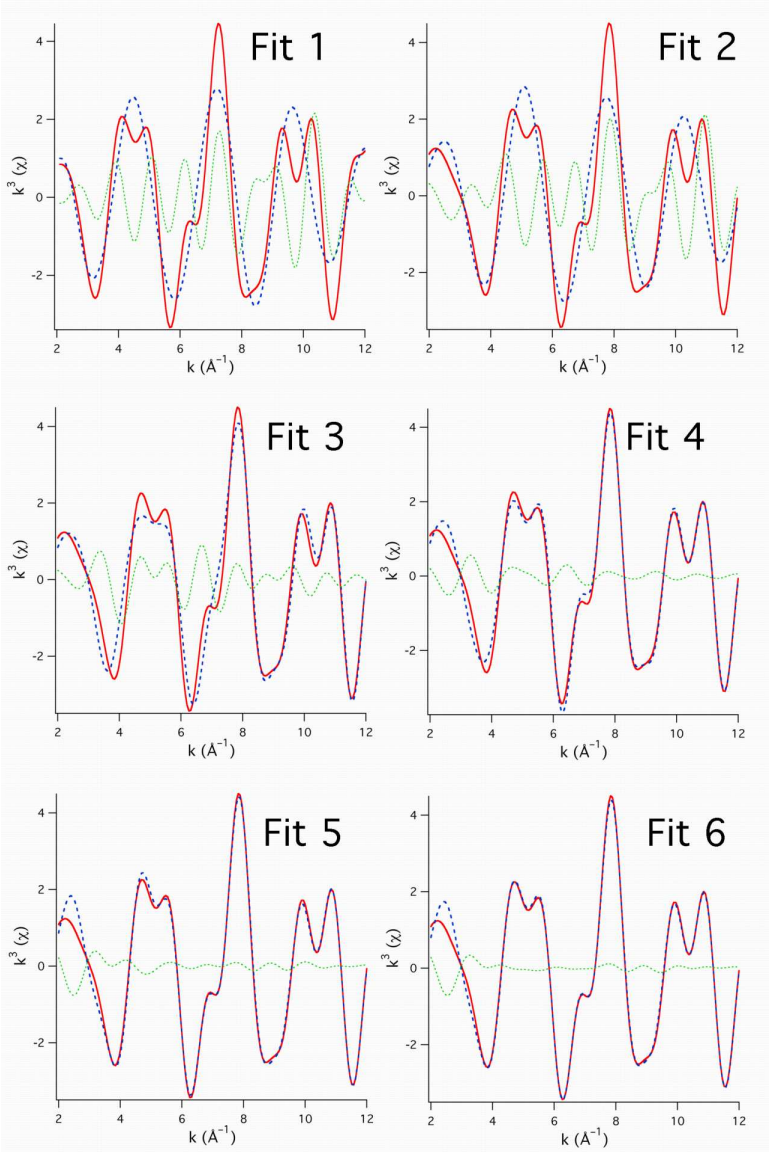

Figure S1. FF EXAFS for different fitting schemes to the AβCu^{II} data. The plot titles correspond to the fits depicted in Table S1 (next page). The data were Fourier transformed from 2.0 to 12.2 Å^{-1} and then back transformed from 1 to 4 Å. The experimental data are given as the red solid line, the fit to the experimental data is given as the dashed blue line, and the difference between the experimental data and the fit is the green dotted line.

Table S1. Trial fits for AβCu^{II}

	Fit 1	Fit 2	Fit 3[a]	Fit 4[b]	Fit 5[c]	Fit 6[b]
N						
shell	4	3	1	3	2	2
n	1.941(9)	1.940(10)	1.93(1)	1.943(5)	1.94(1)	1.913(5)
r (Å)	0.0077(8)	0.0051(13)	0.0033(15)	0.0024(11)	0.002(6)	0.02(5)
σ^2 (A^2)						
O						
shell	-------	1	1	1	1	1
n		2.10(1)	2.07(3)	2.06(1)	2.06(2)	2.06(1)
r (Å)		0.001(1)	0.0011(5)	0.001(2)	0.0025(15)	0.001(1)
σ^2 (A^2)						
N						
shell	-------	-------	-------	-------	1	1
n					1.91(2)	1.87(4)
r (Å)					0.004(2)	0.004(7)
σ^2 (A^2)						
Im						
shell	-------	-------	2	2	2	2
n			1.928(9)	1.932(14)	1.944	1.920(14)
r (Å)			0.0072(13)	0.0053(15)	0.004(7)	0.006(3)
σ^2 (A^2)			3(2)	5(8)	0(2)	7(5)
θ (°)			126(2)	128(6)	134(8)	129(4)
ϕ (°)						
GOF	1.37	1.28	0.67	0.51	0.49	0.49

a) Fit was performed using the Im phase and amplitude function present in *Inorg. Chem.* **2007**, *46*, 710-719, which includes the inner-sphere N scatter as part of the imidazole MS phase and amplitude function.

b) The inner-sphere N scatter as part of the imidazole MS phase and amplitude function was removed, but the distance was allowed to refine freely.

c) The inner-sphere N scatter as part of the imidazole MS phase and amplitude function was removed, but the distance was restrained to the distance of the first inner-sphere N shell.

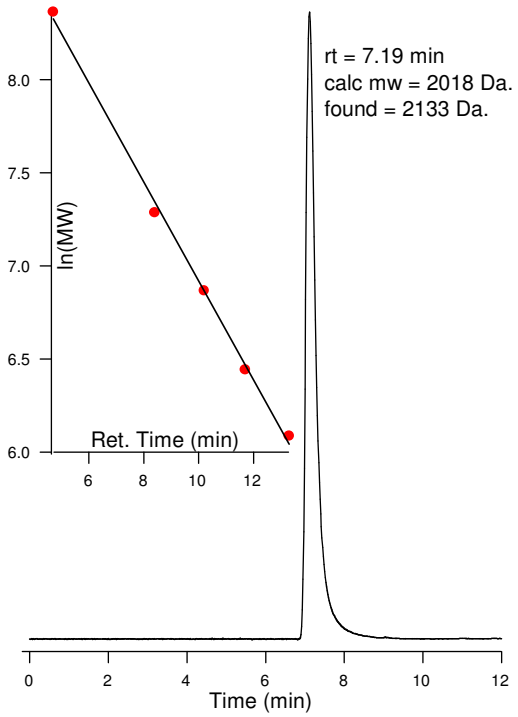

Figure S2. GPC chromatogram (Waters Protein-Pak GPC colum; 7.8 × 300 mm; 60 Å pore size; 5 mM NEM(aq) pH = 7.4) of a solution of $A\beta Cu^{II}$ after exposed to air for 36 hours demonstrating that only monomeric $A\beta Cu^{II}$ can be detected. The inset is the molecular weight calibration plot using the Waters polyethylene glycol standards kit.

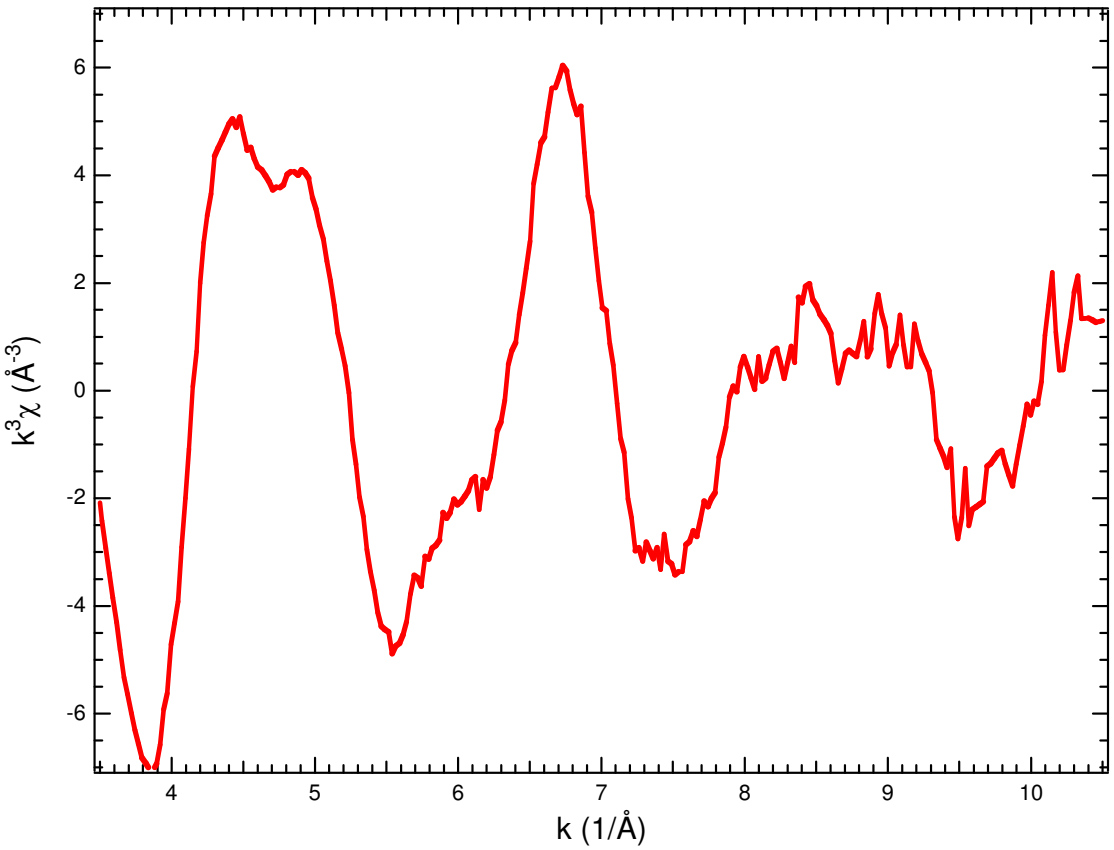

Figure S3: Digitized data from Stellato, F.; Menestrina, G.; Serra, M. D.; Potrich, C.; Tomazzolli, R.; Meyer-Klaucke, W.; Morante, S. *Eur. Biophys. J.* **2006**, 340 reported for Aβ40Cu^{II}. The data presented in Figure 3 from that paper was digitized using the software package GraphDigitizerScout. We note that because of the way in which the figure was digitized the noise, especially at higher *k*, was underestimated in this presentation. Therefore the simulations to the data displayed in Table S2 (next page) are of deceptively higher quality than would have been obtained from the data presented in Morante's study.

Table S2. Re-refinement of the EXAFS data for Aβ40Cu^{II} obtained in Stellato, F.; Menestrina, G.; Serra, M. D.; Potrich, C.; Tomazzolli, R.; Meyer-Klaucke, W.; Morante, S. *Eur. Biophys. J.* **2006**, 340.

	Five Coordinate Fit #1[a]	**Five Coordinate Fit #2**	**Four Coordinate Fit**
N/O Shell			
n[b]	2	3	3
r (Å)	1.96(2)	1.94(1)	1.94(1)
σ^2 (Å^2)	0.006(2)	0.006(1)	0.004(1)
N/O Shell			
n	1	2	1
r (Å)	1.83(4)	2.04(1)	2.04(1)
σ^2 (Å^2)	0.04(1)	0.007(2)	0.003(1)
N/O Shell			
n	1	-----	-----
r (Å)	2.02(3)	-----	-----
σ^2 (Å^2)	0.003(1)	-----	-----
N/O Shell			
n	1	-----	-----
r (Å)	1.91(2)	-----	-----
σ^2 (Å^2)	0.008(2)	-----	-----
Im-Shell			
n	2	2	2
r (Å)[c]	1.957	1.939	1.941
σ^2 (Å^2)	0.002(1)	0.003(1)	0.003(1)
θ	10(4)°	9(2)°	10(1)°
ϕ	133(14)°	132(6)°	132(6)°
Im-Shell			
n	1	-----	-----
r (Å)[c]	1.834	-----	-----
σ^2 (Å^2)	0.03(1)	-----	-----
θ	52(10)°	-----	-----
ϕ	140(18)°	-----	-----
GOF	0.72	0.78	0.64
BVS	2.87	2.71	2.02

a) The number of shells originally used in Stellato, F.; Menestrina, G.; Serra, M. D.; Potrich, C.; Tomazzolli, R.; Meyer-Klaucke, W.; Morante, S. *Eur. Biophys. J.* **2006**, 340. This was done to confirm that we could replicate their original fits with our refinment protocols. Original refinements were: 2 His at 1.94(1) Å (σ^2 = 0.008(3) Å^2); 1 His at 1.85(1) Å (σ^2 = 0.009(4) Å^2); 1 Tyr at 2.00(1) Å (σ^2 = 0.003(1) Å^2); 1 H_2O at 1.91(2) Å (σ^2 = 0.004(2) Å^2). b) Restrained to the nearest whole number from the initial refinement cycle. c) Restrained to the distance from the first shell.

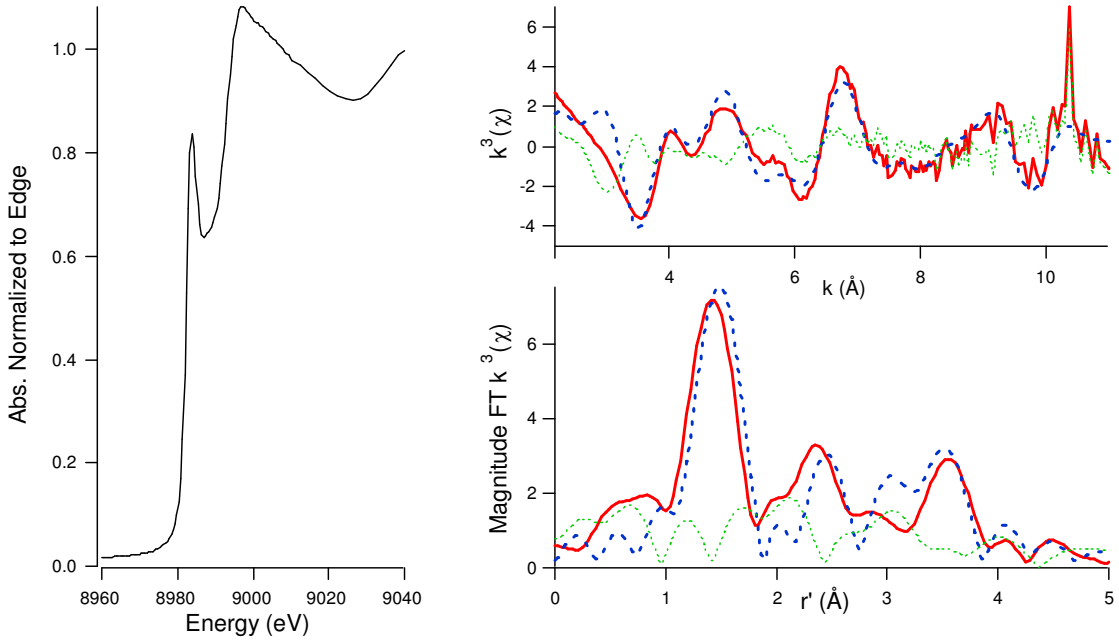

Figure S4. XAS data for reduced Cu(I)Aβ40. The left hand figure depicts the edge spectrum. The top right figure depicts the k^3 EXAFS with the real data as the solid red spectrum, the simulation to the data as the dashed blue spectrum, and the difference spectrum as the dashed green line. The bottom right figure depicts the magnitude FT k^3 EXAFS with the real data as the solid red spectrum, the simulation to the data as the dashed blue spectrum, and the difference spectrum as the dashed green line. The following refinement values were used: Pre-edge peak: 8984.6(2)eV; E_0: 8988.1 eV; N/O shell: n = 2, r = 1.86(1) Å, σ^2 = 0.0042(1) Å^2; imidazole shell: n = 2, r = 1.86 Å (restrained), σ^2 = 0.006(1) Å^2, θ = 6(3)°, ϕ = 133(7)°; GOF = 0.81; BVS = 0.98.

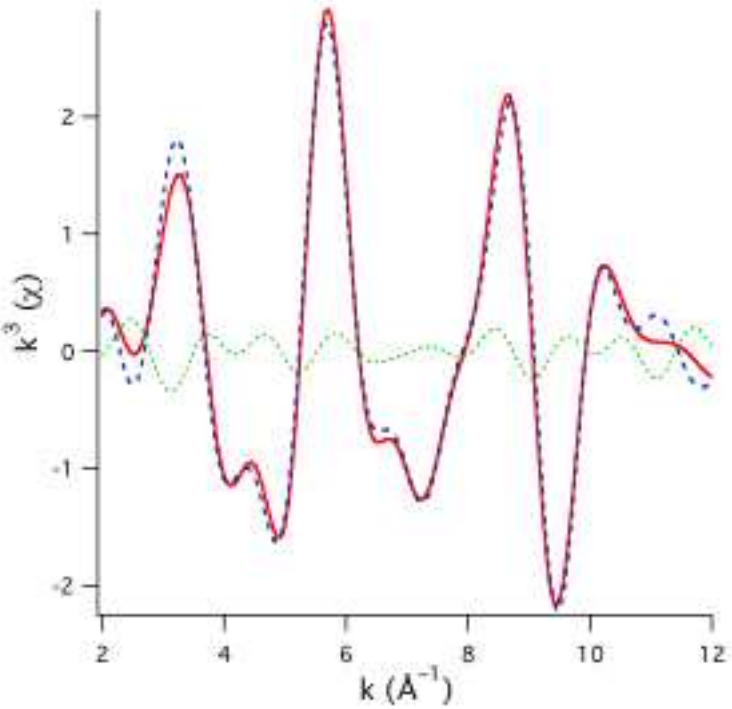

Figure S5. FF EXAFS of AβCu^{I}, alternate fit placing both imidazole scatterers in different shells. The data were Fourier transformed from 2.0 – 12.2 Å^{-1} and back-transformed from 1 – 4 Å. The experimental data is given as the red solid line, the fit to the experimental data is given as the dashed blue line, and the difference between the experimental data and the fit is the green dotted line. The data were modeled using two imidazole and nitrogen scatterers as outlined in the text. N Shell 1: n = 1; r = 1.879(7) Å; σ^2 = 0.0017(4) Å^2. N Shell 2: n = 1; r = 1.871(3) Å; σ^2 = 0.0028(2) Å^2. Imidazole Shell 1: n = 1; r = 1.879 Å (restrained); σ^2 = 0.0013(12) Å^2; θ = 5(3)°; ϕ = 130(2)°. Imidazole Shell 2: n = 1; r = 1.871 Å (restrained); σ^2 = 0.0022(3) Å^2; θ = 2(2)°; ϕ = 130(4)°.

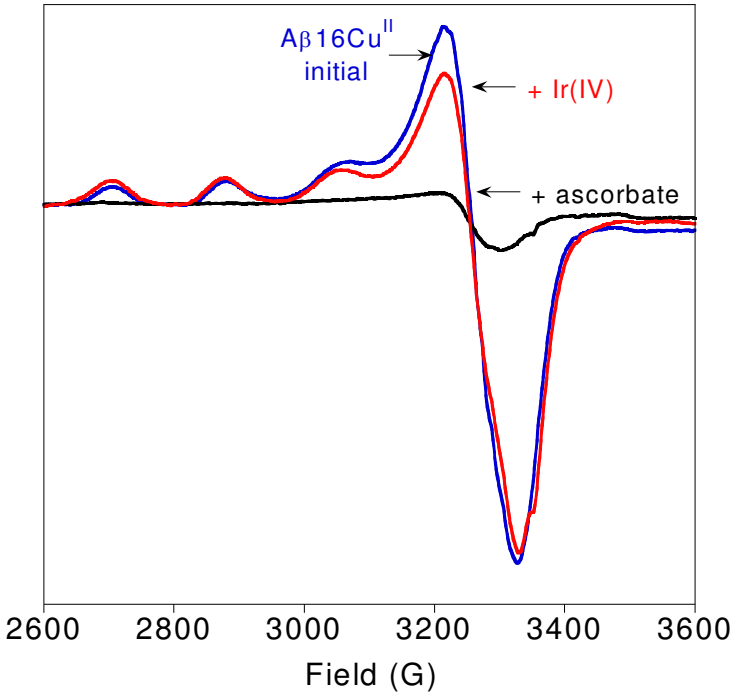

Figure S6: 20 K EPR spectra of the reduction of Aβ16Cu^{II} by ascorbate under inert atmosphere followed by reoxidation using Ir(IV) in air. The Aβ16Cu^{II} complex (109 mM, blue line) is reduced to approximately 5% of its initial concentration by the addition of approximately 2 equiv ascorbate (solid black line). Following the addition of 1 mM $[IrCl_6]^{2-}$, the hyperfine lines for the Aβ16Cu^{II} complex are completely recovered (red line). The stock solution of $K_2[IrCl_6]$ was 19 mM in water. EPR conditions are given in the Materials and Methods Section.

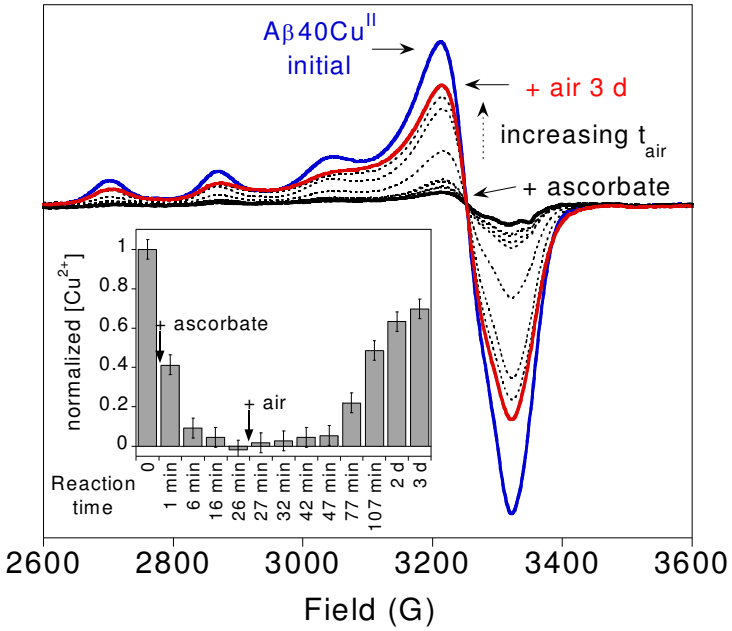

Figure S7: Low-temperature EPR spectra of the reduction of 109 μM Aβ40Cu^{II} (blue) + approximately 2.1 equiv ascorbate (solid black line) followed by addition of air (dotted lines, red line). Inset shows the normalized Aβ40Cu^{II} signal area as a function of the total reaction time. EPR conditions are given in the Materials and Methods Section.

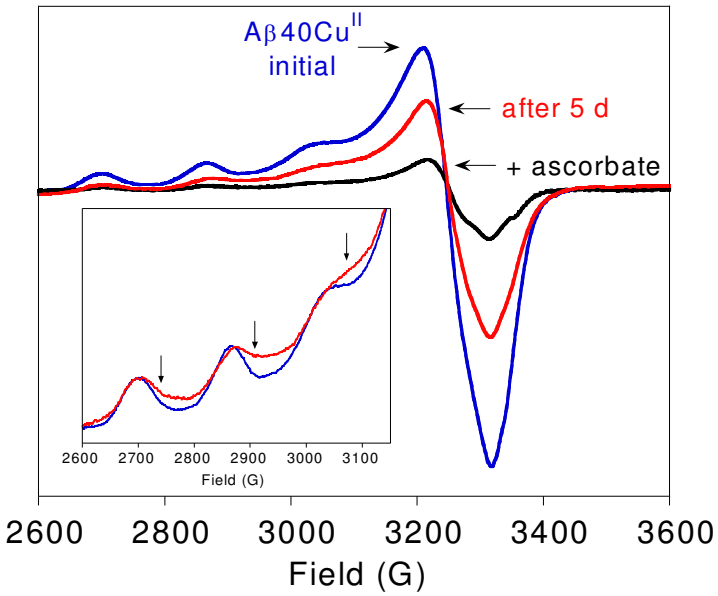

Figure S8: Low-temperature EPR spectra of the reduction of 150 μM Aβ40Cu^{II} (blue) + approximately 4 equiv ascorbate (solid black line) in air over time (red). Inset shows an overlay of the hyperfine regions of the pre and post-ascorbate Cu^{II} EPR signals. The spectrum obtained after 5 days was scaled to facilitate comparison in the inset. The arrows point to changes in the spectral lineshape. EPR conditions are given in the Materials and Methods Section.

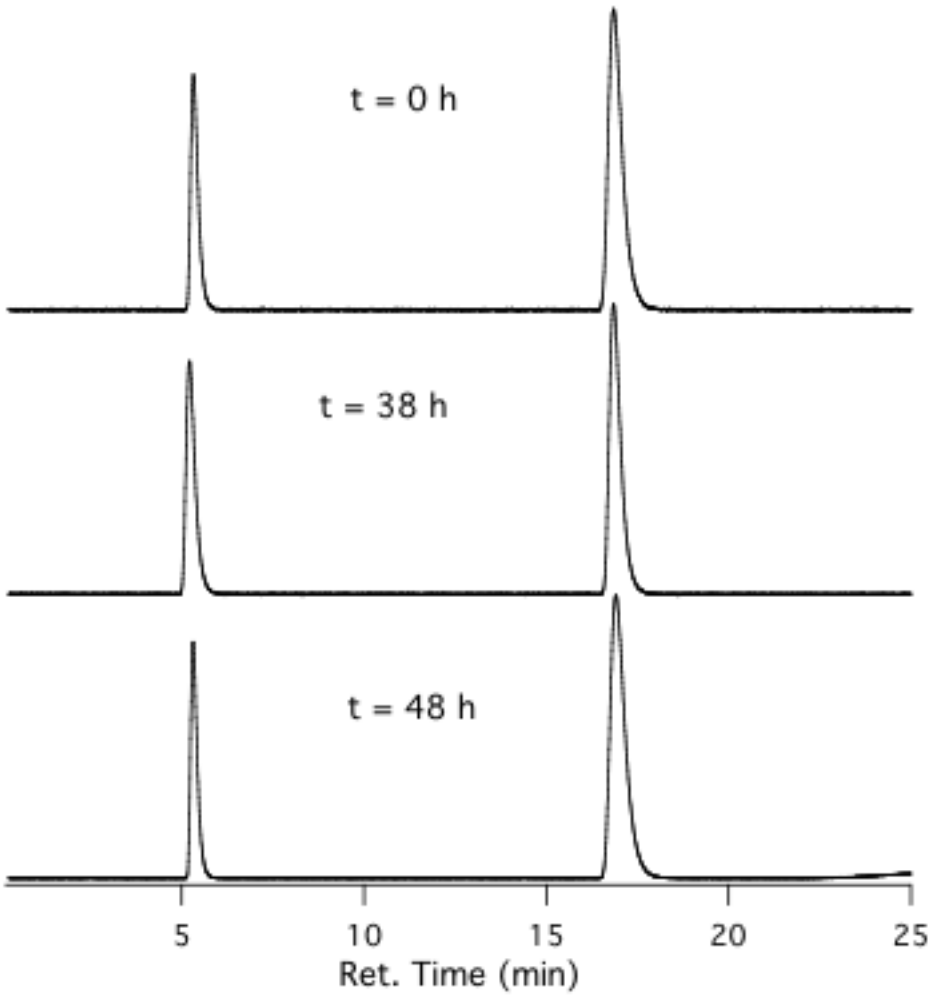

Figure S9. Control chromatograms examining Aβ16Cu^{II} oxidation. The solutions were prepared in a manner similar to that described in the text. The solutions were then bubbled with air and sealed. Samples were monitored by HPLC (25 μL of a 1.00 mL solution) at t = 0 h, 38 h, and 48 h. At time 0 the AβCu^{II}:ref ratio is 2.41, at time 38 h the AβCu^{II}:ref ratio is 2.38 (1.2% reduction in peak area), and at time 48 h the AβCu^{II}:ref ratio is 2.25 (6.7% reduction in peak area). At t = 48 h there is also the appearance of a rise at rt ~ 23 min.

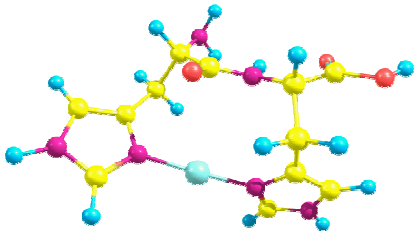

Figure S10. Geometry optimized structure of $[Cu^{I}(HH)]^{+}$. Calculations were performed using the electronic structure package ORCA 2.6.35 employing the B2-PLYP double hybrid functional of Grimme. All atoms were treated with Ahlrichs' TZVP basis set except the Cu and ligating N atoms, which were treated with Ahlrichs' def2-aug-TZVPP basis set. Thresholds used in the geometry optimization procedure were (in a.u.): root-mean-square and maximum forces: 0.0003 and 0.0001, respectively; root-mean-square and maximum gradients: 0.002 and 0.001, respectively. Selected metrical parameters: Cu-N^{1}: 1.871 Å; Cu-N^{2}: 1.873 Å; Im ring 1 (with N^{1}) $\theta = 2.2°$, $\phi = 127.8°$; Im ring 2 (with N^{2}) $\theta = 1.8°$, $\phi = 129.7°$. Coordinates are given in Table S3 (next page).

Table S3. Coordinates for the final GO structure of $[Cu^{I}(HH)]^{+}$.

Cu	0.804000	-1.652000	0.079000
H	3.427000	-2.581000	-1.490000
H	5.459000	-1.040000	-1.484000
C	3.507000	-1.643000	-0.954000
N	4.600000	-0.848000	-0.975000
H	-0.913000	-0.727000	-1.962000
H	-2.666000	-0.682000	-2.219000
C	-1.879000	-0.561000	-1.462000
N	2.571000	-1.093000	-0.175000
O	0.845000	1.148000	-1.608000
C	4.361000	0.256000	-0.180000
C	-2.066000	-1.573000	-0.378000
H	-1.755000	1.520000	-1.933000
N	-0.992000	-2.124000	0.327000
H	5.101000	1.035000	-0.038000
C	-3.223000	-2.143000	0.101000
H	-4.260000	-2.007000	-0.185000
C	3.087000	0.108000	0.316000
C	-1.888000	0.929000	-1.009000
C	-1.496000	-2.996000	1.205000
N	-2.843000	-3.026000	1.092000
C	0.458000	1.469000	-0.479000
H	-0.931000	-3.602000	1.905000
O	-4.266000	1.073000	-1.189000
H	-3.467000	-3.617000	1.636000
N	-0.835000	1.279000	-0.068000
H	2.087000	2.727000	-0.050000
C	-3.215000	1.349000	-0.379000
H	-5.072000	1.415000	-0.745000
C	2.313000	1.000000	1.230000
C	1.427000	2.090000	0.559000
H	1.671000	0.373000	1.875000
H	-1.155000	1.718000	0.798000
H	3.003000	1.536000	1.898000
O	-3.320000	1.873000	0.714000
N	0.865000	2.910000	1.622000
H	0.330000	3.711000	1.287000
H	0.327000	2.392000	2.317000

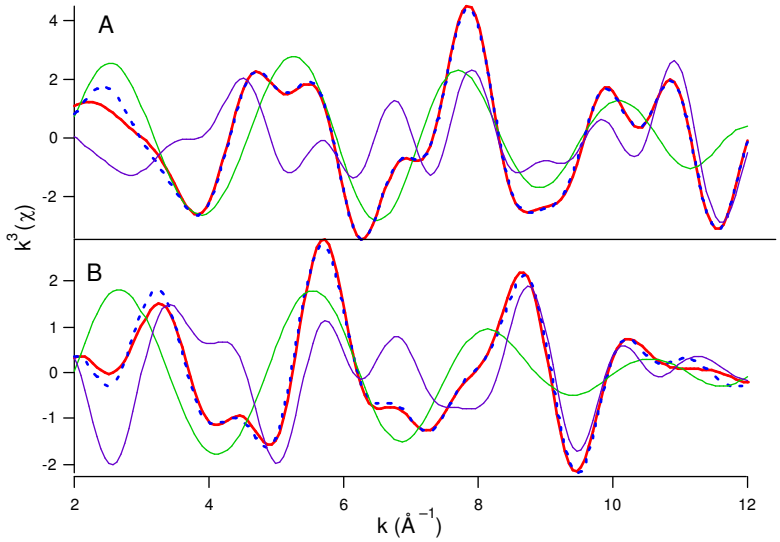

Figure S11. Deconvolution of the MS pathways from the imidazole scatterers (purple) for the inner sphere scatterers (green) from the total simulation (dashed blue) to the EXAFS (experimental data in red: FT from 2 – 12 $Å^{-1}$; backtransformed from 1 – 4 Å). The top are the data for Aβ16Cu^{II} (A) and the bottom are the data from Aβ16Cu^{I} (B).

Complete Reference 51:[1]

(1) Huang, X.; Cuajungco, M. P.; Atwood, C. S.; Hartshorn, M. A.; Tyndall, J. D.; Hanson, G. R.; Stokes, K. C.; Leopold, M.; Multhaup, G.; Goldstein, L. E.; Scarpa, R. C.; Saunders, A. J.; Lim, J.; Moir, R. D.; Glabe, C.; Bowden, E. F.; Masters, C. L.; Fairlie, D. P.; Tanzi, R. E.; Bush, A. I. *J Biol Chem* **1999**, *274*, 37111.